

Phase separation in $\text{Eu}_{0.58}\text{Sr}_{0.42}\text{MnO}_3$ under pressure

W. Zhang, G. J. Liu, J. R. Sun, L. X. Yang, L. D. Yao, F. Y. Li, Z. X. Liu, C. Q. Jin, and R. C. Yu^{a)}

Beijing National Laboratory for Condensed Matter Physics, Institute of Physics, Chinese Academy of Sciences, P. O. Box 603, Beijing 100080, People's Republic of China

(Received 25 May 2007; accepted 12 September 2007; published online 9 November 2007)

Resistivity measurements of $\text{Eu}_{0.58}\text{Sr}_{0.42}\text{MnO}_3$ were carried out at different magnetic fields under ambient pressure and 1 GPa, respectively. The critical temperature T_C of the ferromagnetic metallic state is 128.5 K under 1 GPa and 7 T. The antiferromagnetic insulating phase can be transformed into the ferromagnetic metallic phase by either magnetic field or pressure. Different from the effect of the magnetic field, a plateau is observed in the temperature dependence of the resistivity curve in the lower temperature under pressure, which indicates a phase separation. Magnetic phase diagrams at ambient pressure and 1 GPa are established. © 2007 American Institute of Physics.

[DOI: [10.1063/1.2805647](https://doi.org/10.1063/1.2805647)]

I. INTRODUCTION

Recently, there has been a great deal of attention to colossal magnetoresistance (CMR) manganites ($\text{R}_{1-x}\text{A}_x\text{MnO}_3$, R: rare earth element, A: Ca, Sr, and Ba) because of their interesting electric, magnetic, and structural properties.¹ More and more studies suggest that the ground states of the manganite tend to be intrinsically inhomogeneous due to the presence of strong tendencies toward phase separation, typically involving ferromagnetic (FM) metallic and antiferromagnetic (AFM) insulating domains.²⁻⁴ A lot of experiments with different methods (electron microscopy,³ nuclear magnetic resonance,⁵ resistance and magnetization measurements,⁶ etc.) and theoretical studies⁷ show that the phase separation can be induced by chemical pressure and magnetic field in the CMR materials. Most of those studies are about the manganites with a big radius R ion (R: La, Pr, Nd) for their large bandwidth due to a large tolerance factor. With the variation of the doping level, the compounds $\text{R}_{1-x}\text{A}_x\text{MnO}_3$ can show FM metal, AFM insulator, CE-type charge and orbital ordering phase in different temperature ranges. Sometimes, more than two phases can coexist in the system, which indicates approximately the same energies for different phases.⁸ Thus, a small energy disturbance caused, for example, by temperature, magnetic field,^{9,10} strain,^{11,12} high pressure,¹³⁻¹⁵ etc., can give rise to phase transitions among them. High pressure, as one of thermodynamic parameters, influences the charge, spin, and/or orbital ordering of a sample. For example, $\text{Pr}_{0.7}\text{Ca}_{0.3}\text{MnO}_3$ is a typical CE-type AFM insulator at low temperature and can be transformed from an insulator to a metallic FM phase under a magnetic field of 2 T¹⁶ or a pressure of 0.5 GPa.¹⁷

Different from the ordinary manganite, $\text{Eu}_{1-x}\text{Sr}_x\text{MnO}_3$ always stays at an insulating state for all values of x without a magnetic field^{18,19} due to the narrow bandwidth of the e_g band caused by the small radius of the Eu^{3+} ion. An abrupt shrink about the magnetostriction of $\text{Eu}_{0.58}\text{Sr}_{0.42}\text{MnO}_3$ at 6 K

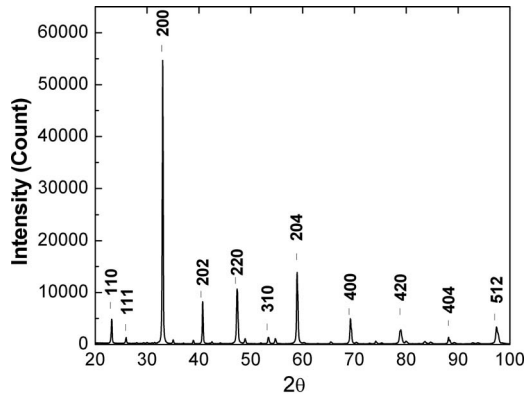
is observed in the process of the increasing field, and a large hysteresis of the magnetostriction indicates that it is a first order phase transition from an insulator to a FM metal.²⁰ Recently, the thermal response of the heat capacity to the paramagnetic-antiferromagnetic (PM-AFM) transition, AFM-FM, and PM-FM transitions in $\text{Eu}_{0.58}\text{Sr}_{0.42}\text{MnO}_3$ are studied under different magnetic fields.²¹ Similar to the magnetic field, pressure can also drive this compound into the FM state from spin glass and/or AFM insulating states.^{22,23} For a thorough understanding of the magnetic and electronic processes in $\text{Eu}_{0.58}\text{Sr}_{0.42}\text{MnO}_3$ in this paper, we performed a systematic study on the combined effects of magnetic field and pressure.

II. EXPERIMENTS

The polycrystalline $\text{Eu}_{0.58}\text{Sr}_{0.42}\text{MnO}_3$ was prepared by the traditional solid-state reaction method. Eu_2O_3 , SrCO_3 , and MnCO_3 were mixed thoroughly in stoichiometric ratios in an agate mortar and calcined at 1000 °C for 24 h, then 1250 °C for 48 h with an intermediate grinding, finally palletized and sintered at 1350 °C for 36 h. Powder x-ray diffractions demonstrated that the sample is a single phase. The lattice parameters are $a=5.4320$ Å, $b=5.4273$ Å, and $c=7.6583$ Å (Ref. 21) with a space group of $Pbnm$.

A clamp-type piston cylinder cell, which utilizes a pressure-transmitting medium composed of 1:1 silicone oil and kerosene, was used to measure the temperature dependence of resistivity under different hydrostatic pressures and magnetic fields, and the mixture of 1:1 silicone oil and kerosene mixture was used as pressure-transmitting medium. Resistivity was measured with the standard four-probe technique. Electrical contacts were established using silver paint on a bar-shaped sample ($\sim 3.7 \times 1.75 \times 0.6$ mm³). The sample temperature was monitored with aluminonickel and chromel thermocouple placed near the sample. In our experiments, the sample was separated from the pressure-transmitting medium by an insulator layer painted on the sample. All the pressure values quoted in this paper were

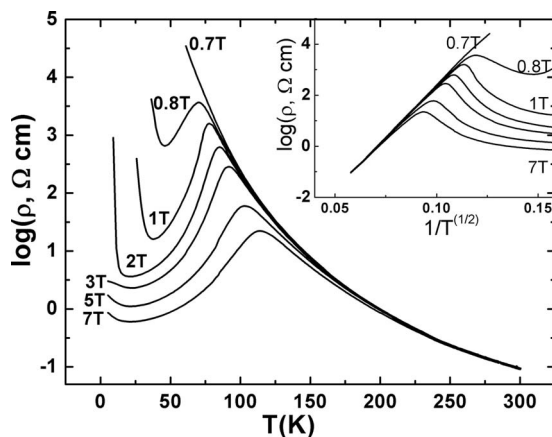
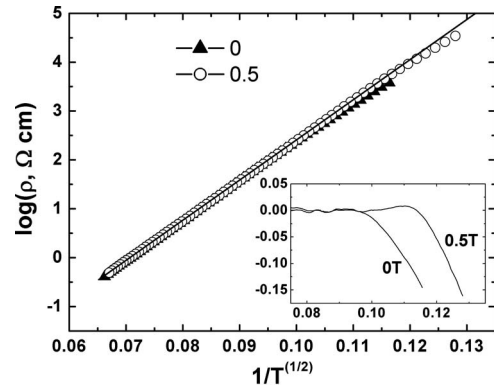
^{a)}Author to whom correspondence should be addressed. Electronic mail: rcyu@aphy.iphy.ac.cn

FIG. 1. X-ray diffraction pattern of $\text{Eu}_{0.58}\text{Sr}_{0.42}\text{MnO}_3$.

measured at room temperature. Resistance versus temperature under magnetic field was measured using a Mag Laboratory System (2000, Oxford, UK).

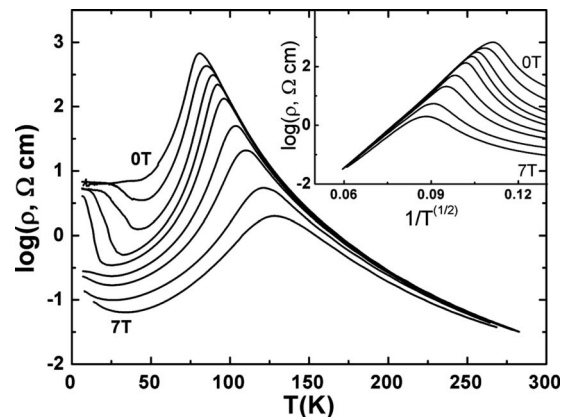
III. RESULTS AND DISCUSSION

In order to check the sample quality, we carried out x-ray diffraction measurements. Figure 1 presents the x-ray diffraction pattern of the $\text{Eu}_{0.58}\text{Sr}_{0.42}\text{MnO}_3$ and all the peaks can be indexed with the space group of $Pbnm$ without any detectable impurities, indicating a high quality single phase of the sample. The characteristics of $\text{Eu}_{0.58}\text{Sr}_{0.42}\text{MnO}_3$ are similar to those reported by Sundaresan *et al.*,²² namely, at zero applied magnetic field, this compound shows a spin glass state below 47 K and a PM state above this temperature. Under low magnetic field $\text{Eu}_{0.58}\text{Sr}_{0.42}\text{MnO}_3$ shows an AFM or a spin glass state in the insulating region at low temperature, a FM state in the metallic region, and paramagnetic state in the insulating region above ~ 100 K. Figure 2 shows the resistivity versus temperature curves at different magnetic fields. Metal-insulator transition (MIT) occurs at ~ 0.8 T, which is less than that reported by Sundaresan *et al.* (1.45 T),²² and the insulator-metal-insulator transitions indicate AFM-FM-PM transitions with increasing temperature, while the sample shows insulating behavior under lower magnetic fields (< 0.7 T). With further increasing mag-

FIG. 2. Temperature dependence of the resistivity at different applied magnetic fields. The inset shows $\log(\rho) \propto (1/T)^{1/2}$ for the paramagnetic insulating state at different magnetic fields.FIG. 3. The semilog plot of resistivity vs $1/T^{1/2}$. The inset is the deviation values of the resistivity curves from the referential straight line.

netic field, there is only one transition from the FM metallic phase to the PM insulating phase. The inset in Fig. 2 presents the semilog plot of resistivity versus $1/T^{1/2}$ obtained under different magnetic fields. It shows that all the curves are linear above the MIT temperature, which suggests a transport mechanism of variable range hopping with a strong electron correlation.^{24,25} Figure 3 shows the semilog plot of resistivity versus $1/T^{1/2}$ obtained under 0 and 0.5 T. The curves are linear at high temperature range, but slightly bend at critical temperatures of ~ 100 and ~ 78 K under 0 and 0.5 T, respectively, which is the same as the point of PM-AFM reported by Liu *et al.*²¹ The inset in Fig. 3 is the deviation values of the resistivity curves from the referential straight line, which shows the critical deviation points more clearly.

In order to investigate the effects of both magnetic field and pressure, we have measured the temperature dependence of resistivity at different magnetic fields under 1 GPa and the results are presented in Fig. 4. Similar to the results reported by others,^{20,23} the MIT can happen under the pressure of 1 GPa without a magnetic field. Interestingly, the MIT temperature increases from ~ 80 K for $H=0$ to 128.5 K for $H=7$ T. The inset of Fig. 4 shows that the transport mechanism is also variable range hopping in the PM state. Similar to the curves, which are resulted from percolative phase separation by chemical pressure³ and theoretical studies,⁷ the

FIG. 4. Temperature dependence of resistivity under 1 GPa at different applied magnetic fields (0, 0.1, 0.2, 0.5, 1, 2, 3, 5, and 7 T). The inset shows $\log(\rho) \propto (1/T)^{1/2}$ for the paramagnetic insulating state at different applied magnetic fields (0, 0.1, 0.2, 0.5, 1, 2, 3, 5, and 7 T).

resistivity curve at zero field in Fig. 4 shows a flat plateau below 45 K. It is interesting that the resistivity values corresponding to the plateau is larger than that of the PM phase in the high temperature range. In Ref. 3, with decreasing y (increasing the content of big radius La ions in $\text{La}_{5/8-y}\text{Pr}_y\text{Ca}_{3/8}\text{MnO}_3$, namely, high chemical pressure), $\text{La}_{5/8-y}\text{Pr}_y\text{Ca}_{3/8}\text{MnO}_3$ changes from an AFM insulating state into the coexistence of FM and AFM states. At $y=0.375$, direct evidence of the two-phase coexistence is confirmed by electron microscopy study, and the temperature dependence of resistivity curve shows a flat plateau in the low temperature range. The residual resistivity corresponding to the plateau is also larger than that of PM phase, which has the same characteristics observed in our experiments. Based on the analyses in Ref. 3, the plateau in the resistivity curve in our experiments can also be explained by the coexistence of FM and AFM components at low temperature. At ambient pressure, none of the resistivity curves show a plateau at low temperature, and the resistivity either increases quickly with decreasing temperature under lower magnetic fields (<2 T), which shows a typical AFM state, or is a small value under larger magnetic fields (>2 T), which shows a FM state. So the inhomogeneities in the form of coexisting competing phases between FM metallic and AFM insulating components are induced by pressure at low temperature. From Fig. 4, the resistivity decreases sharply with increasing temperature in the lower temperature range under low magnetic fields ($H < 1$ T). This suggests the existence of an AFM component considering the fact that the AFM fractions reduce with increasing temperature. Almost the same resistivity values at 5 K indicate that AFM fractions keep unchanging with increasing magnetic field ($0 < H < 1$ T). These phenomena are different from that observed in $\text{La}_{0.5}\text{Ca}_{0.5}\text{MnO}_3$,⁶ which AFM fractions reduce gradually with the increasing field, but keep almost unchanging with the increasing temperature in the lower temperature range. With further increasing temperature, the increase of the resistivity indicates it is a FM state. The large difference in the resistivity between 1 and 2 T at a low temperature indicates they have different states. Under higher magnetic fields (>2 T), the small resistivity values at a low temperature mean that most of the AFM components have been converted to FM by the magnetic field. It should be pointed out that even at high magnetic fields ($H > 2$ T), the resistivity increases slightly with decreasing temperature below about 20 K, which indicates that there is still a small amount of residual AFM phase in the FM background. Comparing Figs. 2 and 4, we can draw a conclusion that both the magnetic field and pressure can depress the antiferromagnetic order and intensify the ferromagnetic order. The difference is that a plateau is observed in the temperature dependence of the resistivity curve in the lower temperature under pressure, which indicates a phase separation, namely, converts some AFM insulating clusters to FM metallic clusters. Figure 5 shows the field dependence of resistivity and it can be seen that the AFM-FM transition is irreversible. At 6 K, the resistivity first reduces slowly with the increasing magnetic field then reduces suddenly at about 1.4 T, which means that the AFM component is converted to a FM component by the magnetic

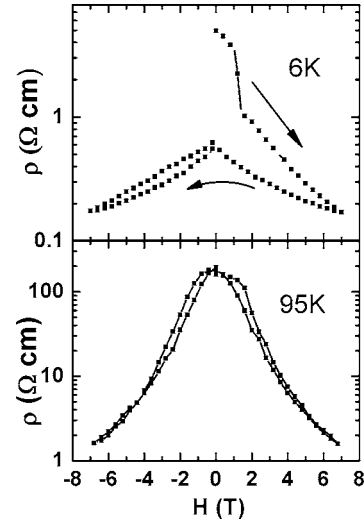


FIG. 5. Resistivity vs magnetic field at 6 and 95 K.

field. After that, the resistivity changes smoothly the under magnetic field, which suggests that none of the FM clusters turn back to the AFM. No sharp change is observed in the resistivity loop with a magnetic field at 95 K (Fig. 5), where only the FM state exists in the sample. The top panel of Fig. 6 shows the resistivity of heating processes at 0.2 T after a zero-field-cooled (ZFC) and field-cooled (FC) (0.2 T), respectively. The difference between ZFC and FC resistivities at low temperature indicates that no AFM component establishing after the FC process, and the hysteretic effect under a 0.2 T magnetic field shown in the bottom panel means that the transformation between the PM phase and the FM phase is a first order phase transition.

We regard the FM transition temperature T_C as the temperature corresponding to the maximum resistance and the AFM transition temperature T_N as the temperature corresponding to the minimum resistance. All T_C and T_N at different magnetic fields under ambient pressure and 1 GPa are shown in Fig. 7. The temperature dependence of T_N under ambient pressure and 1 GPa gives an almost linear relation-

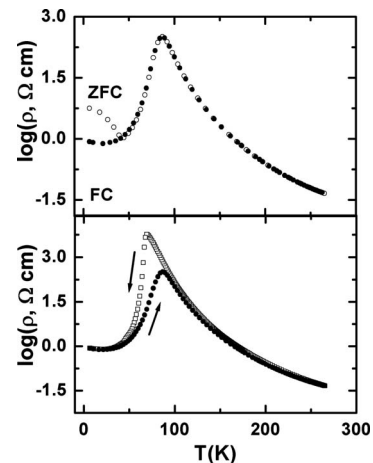


FIG. 6. Resistivity vs temperature under 1 GPa and 0.2 T. The top panel presents heating curves after FC (solid circles) and ZFC (open circles), respectively. The bottom panel presents cooling (open squares) and heating (solid circles) curves under 0.2 T, respectively.

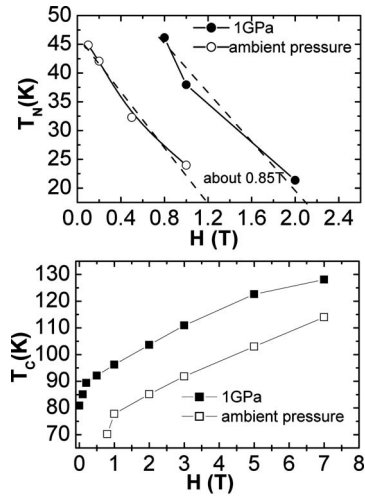


FIG. 7. T_N vs H (top panel) and T_C vs H (bottom panel) under ambient pressure and 1 GPa.

ship. The difference between the two curves of T_N versus the magnetic field is about 0.85 T, while in the FM state, the difference between the two curves of T_C versus the magnetic field is about 3 T, which indicates the different effects of pressure on the FM and AFM states. We establish a magnetic phase diagram in Fig. 8 based on the magnetoresistive data collected under the pressures of $P=0$ and 1 GPa. It shows that the FM region is enlarged by high pressure, demonstrated by the horizontal shift of the PM-FM and FM-AFM boundary, ~ 3 and 0.85 T, respectively, under a pressure of 1 GPa. High pressure drives the AFM ground state into an AFM and FM mixed states and suppresses the AFM state at high temperature.

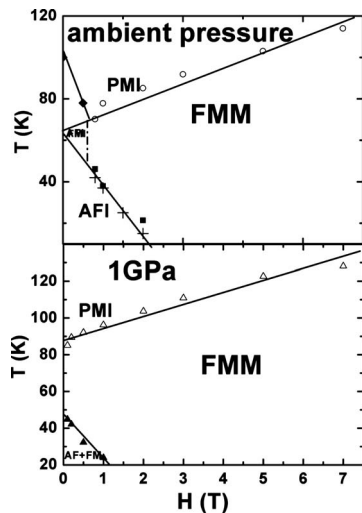


FIG. 8. T - H phase diagram under ambient pressure and 1 GPa. FMM is the ferromagnetic metal, AFI is the antiferromagnetic insulator, and PMI is the paramagnetic insulator. The values at the crosses come from the magnetic measurements reported by Liu *et al.* (Ref. 21).

IV. CONCLUSIONS

The temperature dependence of resistivities of $\text{Eu}_{0.58}\text{Sr}_{0.42}\text{MnO}_3$ at different magnetic fields under ambient pressure and 1 GPa have been studied. The FM metallic state occurs under 1 GPa and zero field and the T_C is 128.5 K under 1 GPa and 7 T. It shows that the FM metallic is enhanced by pressure. Hydrostatic pressure has the same effect as that of the chemical pressure. They both induce a sample to a coexistence of FM and AFM states from AFM insulating state.

ACKNOWLEDGMENTS

This work was supported by the National Natural Science Foundation of China (Grant Nos. 50471053, 10274099, and 50621061) and the State Key Development Program for Basic Research of China (Grant Nos. 2005CB623602 and 2005CB724402).

- ¹ *Colossal Magnetoresistance Oxides*, edited by Y. Tokura (Gordon and Breach, London, 1999); E. Dagotto, T. Hotta, and A. Moreo, Phys. Rep. **344**, 1 (2001).
- ² E. Dagotto, *Nanoscale Phase Separation and Colossal Magnetoresistance* (Springer, Berlin, 2002).
- ³ M. Uehare, S. Mori, C. H. Chen, and S. W. Cheong, Nature (London) **399**, 560 (1999).
- ⁴ S. Mori, C. H. Chen, and S. W. Cheong, Phys. Rev. Lett. **81**, 3972 (1998).
- ⁵ G. Papavassiliou, M. Fardis, M. Belesi, M. Pissas, I. Panagiotopoulos, G. Kallias, D. Niarchos, C. Dimitropoulos, and J. Dolinsek, Phys. Rev. B **59**, 6390 (1999).
- ⁶ M. Roy, J. F. Mitchell, and P. Schiffer, J. Appl. Phys. **87**, 5831 (2000).
- ⁷ M. Mayr, A. Moreo, J. A. Verges, J. Arispe, A. Feiguin, and E. Dagotto, Phys. Rev. Lett. **86**, 135 (2001).
- ⁸ P. M. Woodward, D. E. Cox, T. Vogt, C. N. R. Rao, and A. K. Cheetham, Chem. Mater. **11**, 3528 (1999).
- ⁹ R. Mahendiran, M. R. Ibarra, A. Maignan, F. Millange, A. Arulraj, R. Mahesh, B. Raveau, and C. N. R. Rao, Phys. Rev. Lett. **82**, 2191 (1999).
- ¹⁰ C. Ritter, R. Mahendiran, M. R. Ibarra, L. Morellon, A. Maignan, B. Raveau, and C. N. R. Rao, Phys. Rev. B **61**, R9229 (2000).
- ¹¹ W. Prellier, A. Biswas, M. Rajeswari, T. Venkatesan, and R. L. Greene, Appl. Phys. Lett. **75**, 397 (1999).
- ¹² Q. Qian, T. A. Tyson, C. C. Kao, W. Prellier, J. Bai, A. Biswas, and R. L. Greene, Phys. Rev. B **63**, 224424 (2001).
- ¹³ Y. Moritomo, H. Kuwahara, and Y. Tokura, J. Phys. Soc. Jpn. **66**, 556 (1997).
- ¹⁴ T. H. Arima and K. Nakamura, Phys. Rev. B **60**, R15013 (1999).
- ¹⁵ C. W. Cui, T. A. Tyson, Z. Q. Chen, and Z. Zhong, Phys. Rev. B **68**, 214417 (2003).
- ¹⁶ Y. Tomioka, A. Asamitsu, Y. Moritomo, and Y. Tokura, J. Phys. Soc. Jpn. **64**, 3626 (1995).
- ¹⁷ Y. Moritomo, H. Kuwahara, Y. Tomioka, and Y. Tokura, Phys. Rev. B **55**, 7549 (1997).
- ¹⁸ I. O. Troyanchuk, N. V. Samsonenko, N. V. Kasper, H. Szymczak, and A. Nabialek, Phys. Status Solidi A **160**, 195 (1997).
- ¹⁹ Y. Tadokoro, Y. J. Shan, T. Nakamura, and S. Nakamura, Solid State Ionics **108**, 261 (1998).
- ²⁰ T. Eto, G. Oomi, E. V. Sampathkumaran, A. Sundaresan, M. Kosaka, and Y. Uwatoko, Physica B (Amsterdam) **294-295**, 111 (2001).
- ²¹ G. J. Liu, J. R. Sun, Y. W. Xie, D. J. Wang, C. M. Xiong, H. W. Zhang, T. Y. Zhao, and B. G. Shen, Appl. Phys. Lett. **87**, 182502 (2005).
- ²² A. Sundaresan, A. Maignan, and B. Raveau, Phys. Rev. B **55**, 5596 (1997).
- ²³ I. Kosaka, F. Honda, T. Kagayama, G. Oomi, E. V. Sampathkumaran, and A. Sundaresan, Physica B (Amsterdam) **281-282**, 500 (2000).
- ²⁴ J. M. D. Coey, M. Viret, and S. von Molnar, Adv. Phys. **48**, 167 (1999).
- ²⁵ A. L. Efros and B. I. Shklovskii, J. Phys. C **8**, L49 (1975).